

Preparation and photocatalytic properties of a visible light responsive and magnetically separated photocatalyst of $\gamma\text{-Fe}_2\text{O}_3/\text{SiO}_2/\text{GSs}/\text{TiO}_2$

Deqiang Chen, Yiqun Chen, Yang Li, Shaonan Ye

Key Laboratory of Integrated Regulation and Resource Development on Shallow Lakes, Ministry of Education, College of Environment, Hohai University, Nanjing 210098, People's Republic of China
E-mail: hjycdq@hhu.edu.cn

Published in Micro & Nano Letters; Received on 3rd October 2014; Revised on 16th December 2014; Accepted on 17th March 2015

A graphene sheet (GS) synthesised from natural graphite powder was doped in titanium dioxide (TiO_2) through the sol–gel method to improve the photocatalytic activity and magnetic $\gamma\text{-Fe}_2\text{O}_3/\text{SiO}_2$ particles were added subsequently to improve recycling and reduce the waste of the catalyst. The morphology, microstructure, absorption spectrum and magnetic property of the $\gamma\text{-Fe}_2\text{O}_3/\text{SiO}_2/\text{GSs}/\text{TiO}_2$ composites were characterised via X-ray diffraction, transmission electron microscopy, diffuse-reflectance spectra and a vibrating sample magnetometer, respectively. The result revealed that (i) the nanocrystalline structure of $\gamma\text{-Fe}_2\text{O}_3/\text{SiO}_2/\text{GSs}/\text{TiO}_2$ composites is nearly unchanged compared with pure P25 nanoparticles; (ii) there was a redshift in the absorption edge of the photocatalyst composite; (iii) the photocatalyst composites displayed good superparamagnetism which was in favour of the reclamation of the catalyst; (iv) the adsorption and visible light photocatalytic activity of the composite is enhanced greatly on decomposition of methylene blue and (v) the photocatalysts maintained high photocatalytic activity after being reused several times.

1. Introduction: Nanotitanium dioxide (TiO_2) is considered as one of the most promising photocatalysts for environmental remediation because of its physicochemical properties such as thermal and chemical stability, relatively high photocatalytic activity, low-toxicity and low cost [1–3]. However, there are some obstacles, including the difficulty in separating the suspended TiO_2 from the liquid–solid photocatalytic system and the low quantum yield of TiO_2 under the radiation of sunlight, impeding the large-scale application of TiO_2 photocatalysis in water and air remediation [4, 5]. The immobilisation of TiO_2 on different carriers (glass plates, ceramic membranes etc.) makes it easy to be recycled but the consequent problem is the considerable reduction of photocatalytic activity than that of the suspension system because of the decrease of the effective surface area of the photocatalyst [6–9]. On the other hand, various processes have been proposed via either doping or modification to narrow the bandgap (~ 3.2 eV for the anatase phase) of TiO_2 and enhance the photocatalytic activity under visible light radiation. The modification of TiO_2 with metal or metallic oxide was proved to effectively extend its activation wavelength to the visible region but the metal doping was thermally unstable and easy to cause the recombination of the charge carrier as well [10].

The doping or modifying of titania with nonmetal elements (N, C etc.) was another effective way to obtain a visible light response [11, 12]. In recent years, as a newfound two-dimensional carbon crystal, graphene has been widely investigated because of its unique physical and chemical properties, such as high thermal conductivity [13], high charge carrier mobility at room temperature [14], high specific surface area [15] and complex band structure with conduction and valence bands overlapping for a multi-layer graphene with more than three layers [16]. In view of these attractive attributes, there has been increasing research focusing on coupling graphene with photoactive semiconductors to develop graphene/semiconductor nanocomposites with high photocatalytic performance towards pollution control and abatement [17, 18]. The conjugation of graphene with semiconductor solid particles results in photocatalysts with improved charge separation, reduced recombination of the photogenerated electron–hole pairs, increased specific surface area and an adequate quantity and quality of adsorption sites [18]. Therefore the composite of

graphene and semiconductors, especially TiO_2 , is currently being considered as a potential photocatalyst in air and water purification. Several efforts have been devoted to the combination of graphene and TiO_2 [19–22]. The graphene-based TiO_2 composites exhibit an enhanced photocatalytic activity in comparison with naked TiO_2 .

At the same time, to overcome the difficulty of separating and recovering nanosized titania catalyst from the solution system, the magnetic particles, such as Fe_3O_4 and $\alpha\text{-Fe}_2\text{O}_3$, were introduced as the carrier to synthesise the magnetic TiO_2 which was easy to be reclaimed and will not reduce the activity of the catalyst [23–26]. Fu *et al.* have prepared a series of magnetic photocatalysts from magnetic AFe_2O_4 ($\text{A} = \text{Zn}, \text{Mn}$ and Co) and graphene [27–29]. The obtained samples exhibit great photocatalytic activity, and can be separated easily by applying an external magnetic field. Furthermore, the silica (SiO_2)-isolated layer was added to avoid the electronic interference between the TiO_2 and iron oxide and increase the adhesion of TiO_2 on the carrier [30–32]. Aziz *et al.* [33] have reported a TiO_2 –graphene oxide (GO)-supported $\text{SrFe}_{12}\text{O}_{19}$ ($\text{TiO}_2/\text{GO}/\text{SrFe}_{12}\text{O}_{19}$) photocatalyst, which was synthesised via the solid reaction of SiO_2 -coated $\text{SrFe}_{12}\text{O}_{19}$ with TiO_2 and GO. The synthesised $\text{TiO}_2/\text{GO}/\text{SrFe}_{12}\text{O}_{19}$ exhibited greater ferromagnetic properties and higher visible light absorption.

In this Letter, to combine the advantages of the graphene modification on the promotion of visible light adsorption and iron oxide doping on reuse, a kind of loaded photocatalyst of $\gamma\text{-Fe}_2\text{O}_3/\text{SiO}_2/\text{GSs}/\text{TiO}_2$ was introduced which was expected to remarkably improve the visible light photocatalytic activity and deal with the problem of recycling.

2. Experimental

2.1. Synthesis of photocatalyst

2.1.1 Synthesis of $\gamma\text{-Fe}_2\text{O}_3/\text{SiO}_2$: The magnetic $\gamma\text{-Fe}_2\text{O}_3/\text{SiO}_2$ particles were prepared through a sol–gel method [34]. Briefly, the $\text{FeCl}_2 \cdot 4\text{H}_2\text{O}$ and $\text{FeCl}_3 \cdot 6\text{H}_2\text{O}$ were dissolved in deionised water at a ratio of 2:3 and the mixture was stirred and heated up to 55°C . The pH value of the solution was regulated to 10 by sodium hydroxide solution (1 M) and stirring for 3 h at a constant temperature of 60°C . The resultant sediment was washed several times with anhydrous ethyl alcohol and the $\gamma\text{-Fe}_2\text{O}_3$ was obtained by putting the sediment into the muffle roaster and baking for 1 h at 450°C .

A measure of 1 g of $\gamma\text{-Fe}_2\text{O}_3$ powder was mixed with alcohol (95%, 40 ml) using ultrasonic treatment for 0.5 h. The mixture was further dropped with a mixed solution which contains 4 ml ethyl orthosilicate (TEOS) and 16 ml alcohol (95%) and then was dripped with concentrated ammonia water (10 ml). The resultant particles were stirred for 8 h and the $\gamma\text{-Fe}_2\text{O}_3/\text{SiO}_2$ was obtained after drying.

2.1.2 Synthesis of GO: The GO was synthesised from natural graphite powder using the modified Hummers method [35, 36]. A measure of 0.1 g of GO was added into absolute ethyl alcohol and the GO/EtOH suspension was obtained and 0.2 g of NaBH_4 was added into the suspension after 0.5 h ultrasonic processing. The mixture was stirred for 1 day at room temperature (25°C) and washed with anhydrous alcohol. The graphene sheets (GSs) were obtained after filtering.

2.1.3 Synthesis of $\gamma\text{-Fe}_2\text{O}_3/\text{SiO}_2/\text{GSs}/\text{TiO}_2$: 2 g of GSs was dissolved with anhydrous alcohol and GSs/EtOH was obtained. 10 ml of tetrabutyl orthotitanate (TBOT) was added into the mixture slowly and stirred for 1 day. During stirring, 5 ml of glacial acetic acid and 2 ml of deionised water were added. With the hydrolysis of TBOT, 2.5 g of $\gamma\text{-Fe}_2\text{O}_3/\text{SiO}_2$ particles was added under stirring, and the mixture was stirred for 3 days. Finally, the obtained product was calcined at 400–450°C for 2 h and the complex photocatalyst of $\gamma\text{-Fe}_2\text{O}_3/\text{SiO}_2/\text{GSs}/\text{TiO}_2$ was obtained. The above steps were repeated to get the $\gamma\text{-Fe}_2\text{O}_3/\text{SiO}_2/\text{TiO}_2$ composite without graphene.

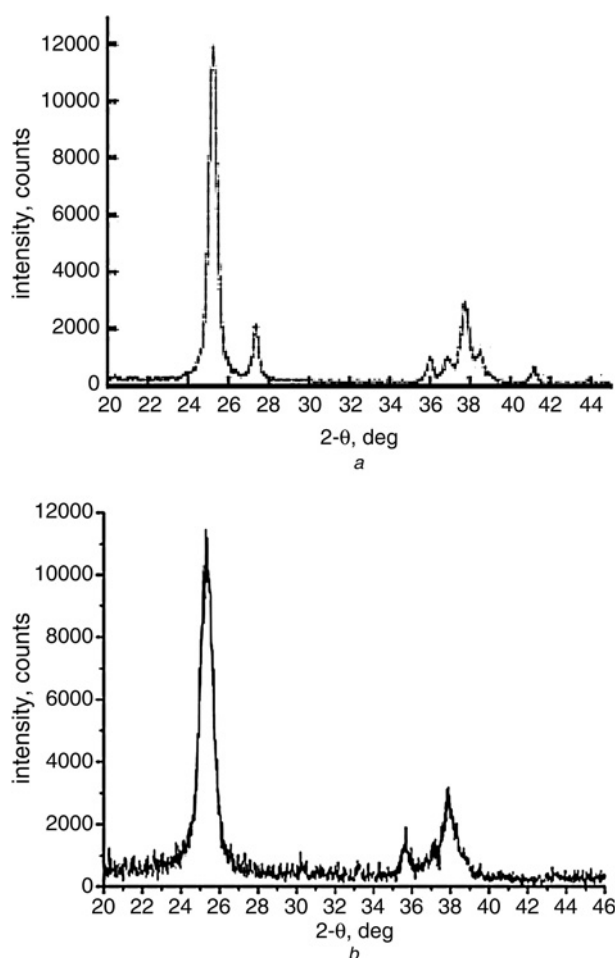


Figure 1 XRD patterns of TiO_2 (Fig. 1a) and $\gamma\text{-Fe}_2\text{O}_3/\text{SiO}_2/\text{GSs}/\text{TiO}_2$ (Fig. 1b)

2.2. Characterisation: The crystal phase of the $\gamma\text{-Fe}_2\text{O}_3/\text{SiO}_2/\text{GSs}/\text{TiO}_2$ composite was conducted using an X-ray diffractometer (X'TRA diffractometer, ARL, Switzerland). The UV–Vis diffuse reflectance spectra was analysed using a UV–Vis-near-infrared spectrophotometer (Cary5000, VARIAN, the USA). For comparison, TiO_2 (P25) nanoparticles (80% anatase + 20% rutile) purchased from Degussa was also measured.

The microstructure of the $\gamma\text{-Fe}_2\text{O}_3/\text{SiO}_2/\text{GSs}/\text{TiO}_2$ composite was observed by a JEM-2100(HR) instrument (JEOL, Japan). The hysteresis loop was measured using a vibrating sample magnetometer (JDM-13T vibrating specimen magnetometer). As a control, the synthetic $\gamma\text{-Fe}_2\text{O}_3/\text{SiO}_2$ was also measured.

Methylene concentration was determined by its absorbance at 540 nm using a UV–Vis spectrophotometer (UV-7504, China).

2.3. Adsorption experiments: The adsorbability of the photocatalysts was evaluated by adsorption of methyl blue (MB). Twenty milligrams of photocatalysts was dispersed into 500 ml of water solution containing 20 mg l^{-1} MB, and then the mixture was stirred incessantly at room temperature in the dark. The concentration of MB was measured by a UV–Vis spectrophotometer every 15 min.

2.4. Photocatalytic degradation experiments: A 125 W high-pressure mercury lamp and a cut-off filter ($\lambda > 400 \text{ nm}$) were used as the light source for photocatalytic reaction. The photocatalytic activity of the $\gamma\text{-Fe}_2\text{O}_3/\text{SiO}_2/\text{GSs}/\text{TiO}_2$ composite was assessed by the decomposition of MB. Twenty milligrams of photocatalysts was dispersed into 500 ml of water solution containing 20 mg l^{-1} MB, and then the mixture was stirred constantly under light with a distance of 25 cm. The concentration of MB was measured by a UV–Vis spectrophotometer every 15 min.

To investigate the photodegradation efficiency of reused photocatalysts, the composites were recycled using a magnetic field, cleaned by distilled water and dried at 100°C for 4–5 h. The photocatalysts were reused three times and the photocatalytic activity was evaluated by decomposition of MB.

3. Results and discussion

3.1. Characterisation

3.1.1 X-ray diffraction (XRD): The XRD spectra of commercial TiO_2 (P25) and $\gamma\text{-Fe}_2\text{O}_3/\text{SiO}_2/\text{GSs}/\text{TiO}_2$ composite are presented in Fig. 1. Clearly, both materials exhibit similar XRD patterns. As shown in Fig. 1, the series of strong peaks at 2θ of 25.2, 37.76 and 38.52 were, respectively, corresponding to the (101), (004) and (112) crystal planes of the anatase phase. These signals were indicative of the dominant anatase phase in both composites which was generally recognised by higher photocatalytic activity than the rutile form. Remarkably, no relevant peaks of Fe_2O_3 and SiO_2 graphene were observed in the spectra of the $\text{Fe}_2\text{O}_3/\text{SiO}_2/\text{GSs}/\text{TiO}_2$ composite because of the extremely small amounts of

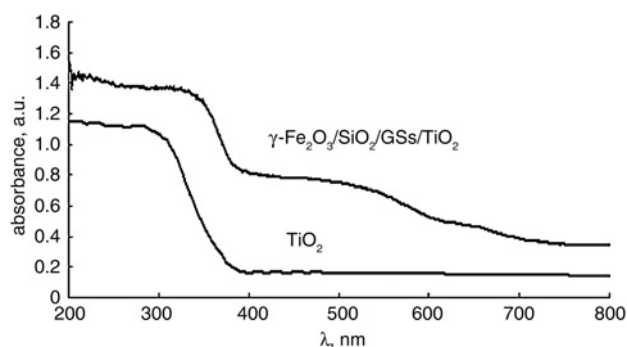


Figure 2 DRS of the TiO_2 and $\gamma\text{-Fe}_2\text{O}_3/\text{SiO}_2/\text{GSs}/\text{TiO}_2$

Fe_2O_3 and SiO_2 in the composite. Moreover, no diffraction peak of graphene was discerned in the XRD patterns of the composites. This may be attributed to the overlap of the diffraction peak between graphene and TiO_2 at 2θ of 25.2° [37].

According to the Scherrer formula [38], the mean particles of P25 and $\gamma\text{-Fe}_2\text{O}_3/\text{SiO}_2/\text{GSS}/\text{TiO}_2$ were calculated to be 21 and 10 nm, respectively. The results indicated that the composites had larger specific surface area than that of P25 which was conducive to photocatalytic performance.

3.1.2 Diffuse-reflection spectra (DRS): Fig. 2 shows the UV-Vis absorption spectra of TiO_2 (P25) and $\gamma\text{-Fe}_2\text{O}_3/\text{SiO}_2/\text{GSS}/\text{TiO}_2$ composites. Obviously, the $\gamma\text{-Fe}_2\text{O}_3/\text{SiO}_2/\text{GSS}/\text{TiO}_2$ composite displayed not only redshift in the absorption edge but also a strong absorption in the visible light range. The results demonstrated the effect of graphene on the optical characteristics of composites in which graphene narrowed the bandgap of TiO_2 . Similar to the case of TiO_2 -CNTs, C-doped TiO_2 or chemically converted TiO_2 graphene composites, the phenomena in this Letter could be ascribed to the formation of the Ti-O-C bond in the prepared composites which shifted up the valence band edge and reduced the bandgap [39, 40]. Furthermore, the significant improvement of visible light absorbance of the composite could also be attributed to the doping of graphene which effectively improved the photocurrent of the composites [41].

3.1.3 Transmission electron microscopy (TEM): Fig. 3 shows the TEM image of $\gamma\text{-Fe}_2\text{O}_3/\text{SiO}_2$ and $\gamma\text{-Fe}_2\text{O}_3/\text{SiO}_2/\text{GSS}/\text{TiO}_2$. Compared with the $\gamma\text{-Fe}_2\text{O}_3/\text{SiO}_2$ particles, the prepared titania compound photocatalysts had a regular and orderly structure. As shown in Fig. 3b, the TiO_2 nanoparticles were mostly covered with graphene nanosheets which effectively enlarged the specific surface and was advantageous to the molecular adsorption and electronic transmission in the process of photocatalytic reaction. According to the TEM image, the average particle size of $\gamma\text{-Fe}_2\text{O}_3/\text{SiO}_2/\text{GSS}/\text{TiO}_2$ was about 10 nm, which was in concordance with the results calculated from the XRD spectra.

3.1.4 Hysteresis loop analysis: Fig. 4 illustrates the hysteresis loops of $\gamma\text{-Fe}_2\text{O}_3/\text{SiO}_2$ and $\gamma\text{-Fe}_2\text{O}_3/\text{SiO}_2/\text{GSS}/\text{TiO}_2$. The saturation magnetisation of the $\gamma\text{-Fe}_2\text{O}_3/\text{SiO}_2/\text{GSS}/\text{TiO}_2$ composite was 3.48 emu/g compared with 32.73 emu/g of $\gamma\text{-Fe}_2\text{O}_3/\text{SiO}_2$. The decrease of saturation magnetisation in the prepared titania compound may be related to the reduction of the $\gamma\text{-Fe}_2\text{O}_3/\text{SiO}_2$ content by 10%.

As shown in Fig. 4, there was no magnetic hysteresis in both materials. When external magnetic field is $H = 0$, the residual magnetisation $M_r = 0$ and the coercivity $H_c = 0$. The prepared titania composite displayed good superparamagnetism that could be attributable to the isolation of SiO_2 coatings during the calcining process. This makes the composites easy to be recovered under an external magnetic field and redisperse in the reaction system when the

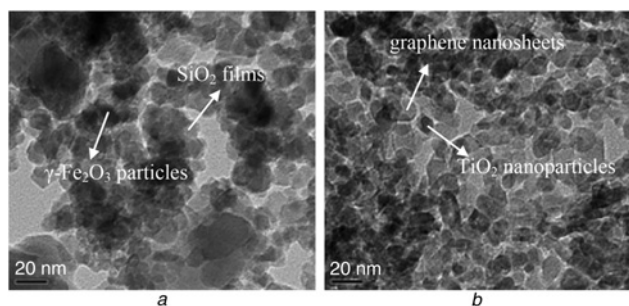


Figure 3 TEM image of $\gamma\text{-Fe}_2\text{O}_3/\text{SiO}_2$ (Fig. 3a) and $\gamma\text{-Fe}_2\text{O}_3/\text{SiO}_2/\text{GSS}/\text{TiO}_2$ (Fig. 3b)

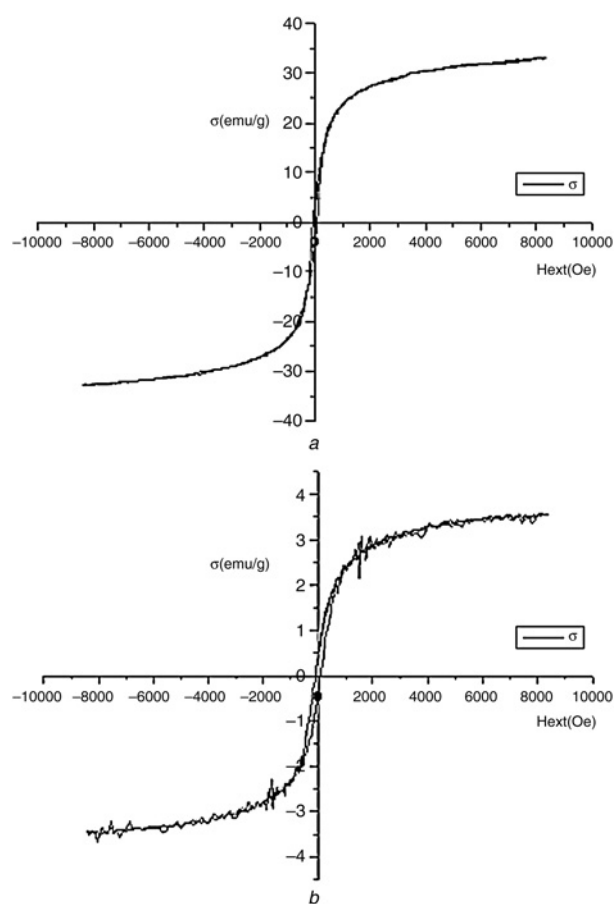


Figure 4 Hysteresis loops of $\gamma\text{-Fe}_2\text{O}_3/\text{SiO}_2$ (Fig. 4a) and $\gamma\text{-Fe}_2\text{O}_3/\text{SiO}_2/\text{GSS}/\text{TiO}_2$ (Fig. 4b)

magnetic field was removed and avoids the magnetic agglomeration of composites itself.

3.2. Photocatalytic performance of $\gamma\text{-Fe}_2\text{O}_3/\text{SiO}_2/\text{GSS}/\text{TiO}_2$

3.2.1 Adsorbability of $\gamma\text{-Fe}_2\text{O}_3/\text{SiO}_2/\text{GSS}/\text{TiO}_2$: The photocatalytic performance was significantly dependent on the adsorbability of the catalysts. Fig. 5 displays the adsorption capacity of the $\gamma\text{-Fe}_2\text{O}_3/\text{SiO}_2$ and $\gamma\text{-Fe}_2\text{O}_3/\text{SiO}_2/\text{GSS}/\text{TiO}_2$ composites. For the $\gamma\text{-Fe}_2\text{O}_3/\text{SiO}_2/\text{GSS}/\text{TiO}_2$ composite, about 10% of MB solutions was adsorbed after 75 min; in contrast, only 2% of MB solutions was adsorbed for the $\gamma\text{-Fe}_2\text{O}_3/\text{SiO}_2/\text{TiO}_2$ compound. This improvement was attributed to the introduction of graphene. The crumpled surface of the graphene could provide a large surface area which

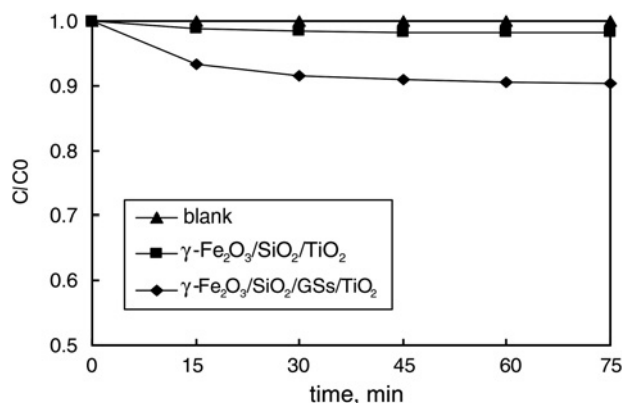


Figure 5 Adsorbability of $\gamma\text{-Fe}_2\text{O}_3/\text{SiO}_2$ and $\gamma\text{-Fe}_2\text{O}_3/\text{SiO}_2/\text{GSS}/\text{TiO}_2$

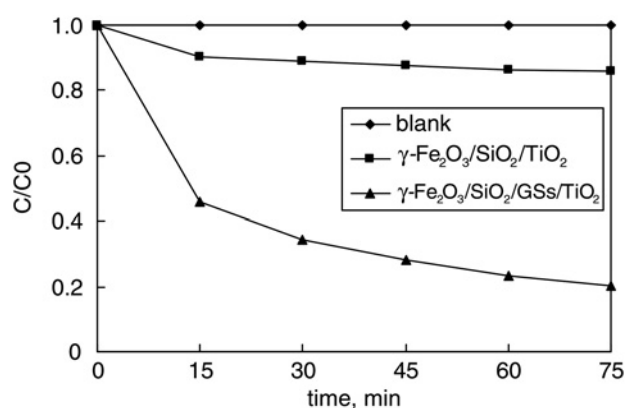


Figure 6 Decompositions of MB by $\gamma\text{-Fe}_2\text{O}_3/\text{SiO}_2$ and $\gamma\text{-Fe}_2\text{O}_3/\text{SiO}_2/\text{GSs}/\text{TiO}_2$

would favour larger contact interfaces between TiO_2 particles and the graphene nanosheets, thus promoting the adsorbability of catalysts [42, 43].

3.2.2 Photocatalytic activity of $\gamma\text{-Fe}_2\text{O}_3/\text{SiO}_2/\text{GSs}/\text{TiO}_2$: Fig. 6 shows the decompositions of MB under visible light by the $\gamma\text{-Fe}_2\text{O}_3/\text{SiO}_2$ and $\gamma\text{-Fe}_2\text{O}_3/\text{SiO}_2/\text{GSs}/\text{TiO}_2$ composites. The degradation rates of MB were 14 and 80% by $\gamma\text{-Fe}_2\text{O}_3/\text{SiO}_2/\text{TiO}_2$ and $\gamma\text{-Fe}_2\text{O}_3/\text{SiO}_2/\text{GSs}/\text{TiO}_2$, respectively. Obviously, the doping of graphene improved the photocatalytic performance of TiO_2 . The enhanced photocatalytic performance can be attributed to the introduction of graphene, which had an extraordinary microscopic structure and a great electronic property. First, the involvement of graphene nanosheets can efficiently prevent the stacking of TiO_2 nanoparticles which can lead to the decrease of photoactivity in the photoreaction [44]. Secondly, the graphene possesses a remarkable electrical transport property. In the $\gamma\text{-Fe}_2\text{O}_3/\text{SiO}_2/\text{GSs}/\text{TiO}_2$ composite, the graphene played a role of conducting electrons which can accelerate the photogenerated electron transfer from TiO_2 to the surface of graphene and retard effectively the recombination of electron-hole pairs over the composite, thus promoting the photocatalytic efficiency of catalysts [45, 46]. Furthermore, according to the above-mentioned result, the doping of graphene could increase the specific surface area of the composite, thus offering more photocatalytic reaction centres and improving the photoactivity of catalysts.

3.2.3 Photocatalytic performance of reused photocatalyst: Fig. 7 displays the decompositions of MB in the visible light by photocatalysts being reused several times. After being recycled three times, the photocatalysts maintained high photocatalytic activity. The

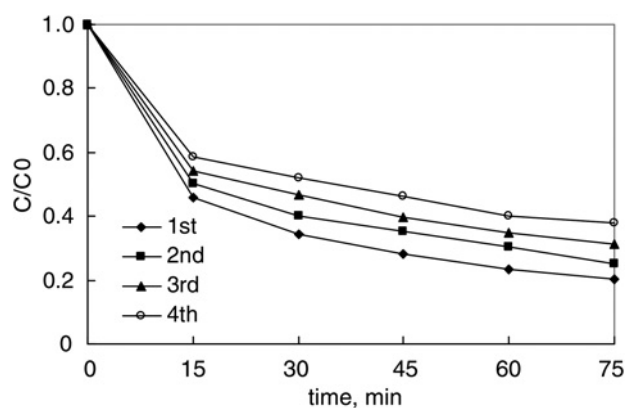


Figure 7 Decompositions of MB by reused $\gamma\text{-Fe}_2\text{O}_3/\text{SiO}_2/\text{GSs}/\text{TiO}_2$

decomposition rate of MB was still up to 62.2%, compared with 80% by the initial composites. The stable photocatalytic activity of the composites could be ascribed to the formation of Ti-O-C bonds between TiO_2 and graphene, as described in the DRS result, which made the photocatalyst not easily inactive during the degradation of MB. The decrease of the degradation rate may be due to the small amount of photocatalysts lost and the residual of MB attached to the catalyst particles which affected the adsorption of visible light of TiO_2 and reduced the photocatalytic activity.

4. Conclusion: A $\gamma\text{-Fe}_2\text{O}_3/\text{SiO}_2/\text{GSs}/\text{TiO}_2$ composite with remarkable visible light photocatalytic activity and a reusable property was synthesised using a colloidal blending method. During photocatalysis, graphene played a key role in the aspects of adsorption of MB molecules, the separation of electron-hole pairs and the improvement of the visible light absorption because of C-doping in the TiO_2 surface. Furthermore, the prepared photocatalysts exhibited good superparamagnetism and stable photocatalytic activity after being reused several times because of the doping of $\gamma\text{-Fe}_2\text{O}_3$.

5. Acknowledgments: This work was financially supported by the National Natural Science Foundation of China (no. 51309081), the Fundamental Research Funds for the Central Universities (2010B05314) and by a Project funded by the Priority Academic Program Development of Jiangsu Higher Education Institutions.

6 References

- [1] Mor G.K., Prakasam H.E., Varghese O.K., Shankar K., Grimes C.A.: 'Vertically oriented Ti-Fe-O nanotube array films: toward a useful material architecture for solar spectrum water photoelectrolysis', *Nano Lett.*, 2007, **7**, (8), pp. 2356–2364
- [2] Chiarello G.L., Selli E., Forni L.: 'Photocatalytic hydrogen production over flame spray pyrolysis-synthesised TiO_2 and Au/TiO_2 ', *Appl. Catal. B, Environ.*, 2008, **84**, (1–2), pp. 332–339
- [3] Seger B., Kamat P.V.: 'Fuel cell geared in reverse: photocatalytic hydrogen production using a $\text{TiO}_2/\text{Nafion}/\text{Pt}$ membrane assembly with no applied bias', *J. Phys. Chem. C*, 2009, **113**, pp. 18946–18952
- [4] Chen X., Mao S.S.: 'Titanium dioxide nanomaterials: synthesis, properties, modifications, and applications', *Chem. Rev.*, 2007, **107**, pp. 2891–2959
- [5] Burda C., Chen X., Narayanan R., El-Sayed M.A.: 'Chemistry and properties of nanocrystals of different shapes', *Chem. Rev.*, 2005, **105**, pp. 1025–1102
- [6] Robert D., Piscopo A., Heintz O., Weber J.V.: 'Photocatalytic detoxification with TiO_2 supported on glass-fiber by using artificial and natural light', *Catal. Today*, 1999, **54**, pp. 291–296
- [7] Hsien Y.H., Chang C.F., Chen Y.H., Cheng S.: 'Photodegradation of aromatic pollutants in water over TiO_2 supported on molecular sieves', *Appl. Catal. B, Environ.*, 2001, **31**, (4), pp. 241–249
- [8] Ma Y., Qiu J.B., Cao Y.A., Guan Z.S., Yao J.N.: 'Photocatalytic activity of TiO_2 films grown on different substrates', *Chemosphere*, 2001, **44**, (5), pp. 1087–1092
- [9] Stafford U., Gray K., Kamat A.P.V.: 'Radiolytic and TiO_2 -assisted photocatalytic degradation of 2,4-chlorophenol: a comparative study', *J. Phys. Chem.*, 1994, **98**, (25), pp. 6343–6351
- [10] Choi W.Y., Termin A., Hoffmann M.R.: 'The role of metal-ion dopants in quantum-sized TiO_2 -correlation between photoreactivity and charge-carrier recombination dynamics', *J. Phys. Chem.*, 1994, **98**, (51), pp. 13669–13679
- [11] Asahi R., Morikawa T., Ohwaki T., Aoki K., Taga Y.: 'Visible-light photocatalysis in nitrogen-doped titanium oxides', *Science*, 2001, **293**, (5528), pp. 269–271
- [12] Park J.H., Kim S., Bard A.J.: 'Novel carbon-doped TiO_2 nanotube arrays with high aspect ratios for efficient solar water splitting', *Nano Lett.*, 2006, **6**, (1), pp. 24–28
- [13] Balandin A.A., Ghosh S., Bao W., ET AL.: 'Superior thermal conductivity of single-layer graphene', *Nano Lett.*, 2008, **8**, (3), pp. 902–907
- [14] Bolotin K.I., Sikes K.J., Jiang Z., ET AL.: 'Ultrahigh electron mobility in suspended graphene', *Solid-State Commun.*, 2008, **146**, pp. 351–355

- [15] Peter S., Rainer W., Ralf T., Rolf M.: 'Functionalized graphenes and thermoplastic nanocomposites based upon expanded graphite oxide', *Macromol. Rapid Commun.*, 2009, **30**, (4–5), pp. 316–327
- [16] Klintonberg M., Lebegue S., Ortiz C., Sanyal B., Fransson J., Eriksson O.: 'Evolving properties of two-dimensional materials: from graphene to graphite', *J. Phys., Condens. Matter*, 2009, **21**, (33), pp. 550–552
- [17] Zhang N., Zhang Y., Xu Y.J.: 'Recent progress on graphene-based photocatalysts: current status and future perspectives', *Nanoscale*, 2012, **4**, pp. 5792–5813
- [18] Han L., Wang P., Dong S.: 'Progress in graphene-based photoactive nanocomposites as a promising class of photocatalyst', *Nanoscale*, 2012, **4**, pp. 5814–5825
- [19] Liang Y., Wang H., Casalongue H.S., Chen Z., Dai H.: 'TiO₂ nanocrystals grown on graphene as advanced photocatalytic hybrid materials', *Nano Res.*, 2010, **3**, pp. 701–705
- [20] Liu J., Bai H., Wang Y., Liu Z., Zhang X., Sun D.D.: 'Self-assembling TiO₂ nanorods on large graphene oxide sheets at a two-phase interface and their anti-recombination in photocatalytic applications', *Adv. Funct. Mater.*, 2010, **20**, pp. 4175–4181
- [21] Chen C., Cai W., Long M., *ET AL.*: 'Synthesis of visible-light responsive graphene oxide/TiO₂ composites with p/n heterojunction', *ACS Nano*, 2010, **4**, pp. 6425–6432
- [22] Pan X., Zhao Y., Liu S., Korzeniewski C., Wang S., Fan Z.: 'Comparing graphene–TiO₂ nanowire and graphene–TiO₂ nanoparticles composite photocatalysts', *ACS Appl. Mater. Interfaces*, 2012, **4**, pp. 3944–3950
- [23] Chen F., Zhao J.: 'Preparation and photocatalytic properties of a novel kind of loaded photocatalyst of TiO₂/SiO₂/γ-Fe₂O₃', *Catalyst Lett.*, 1999, **58**, pp. 245–252
- [24] Chen F., Xie Y., Zhao J., Lu G.: 'Photocatalytic degradation of dyes on a magnetically separated photocatalyst under visible and UV irradiation', *Chemosphere*, 2001, **44**, pp. 1159–1168
- [25] Ao Y., Xu J., Fu D., Yuan C.: 'A simple route for the preparation of anatase titania-coated magnetic porous carbons with enhanced photocatalytic activity', *Carbon*, 2008, **46**, pp. 596–603
- [26] Ao Y., Xu J., Fu D., Yuan C.: 'Photocatalytic degradation of X-3B by titania-coated magnetic activated carbon under UV and visible irradiation', *J. Alloys Compd.*, 2009, **471**, pp. 33–38
- [27] Fu Y., Wang X.: 'Magnetically separable ZnFe₂O₄-graphene catalyst and its high photocatalytic performance under visible light irradiation', *Ind. Eng. Chem. Res.*, 2011, **50**, pp. 7210–7218
- [28] Fu Y., Xiong P., Chen H., Sun X., Wang X.: 'High photocatalytic activity of magnetically separable manganese ferrite-graphene hetero-architectures', *Ind. Eng. Chem. Res.*, 2012, **51**, pp. 725–731
- [29] Fu Y., Chen H., Sun X., Wang X.: 'Combination of cobalt ferrite and graphene: high-performance and recyclable visible-light photocatalysis', *Appl. Catal. B, Environ.*, 2012, **111–112**, pp. 280–287
- [30] Donia B., Rose A.: 'Implications of heat treatment on the properties of a magnetic iron oxide-titanium dioxide photocatalyst', *Mater. Sci. Eng., B*, 2002, **94**, (1), pp. 71–81
- [31] Beydoun D., Amal R., Low G.K.C., McEvoy S.: 'Novel photocatalyst: titania-coated magnetite activity and photodissolution', *J. Phys. Chem. B.*, 2000, **104**, (18), pp. 4387–4396
- [32] Donia B., Rose A.I., Gary L., Stephen M.: 'Occurrence and prevention of photodissolution at the phase junction of magnetite and titanium dioxide', *J. Mol. Catal. A, Chem.*, 2002, **180**, (1–2), pp. 193–200
- [33] Aziz A.A., Yau Y.H., Puma G.L., Fischer C., Ibrahim S., Pichiah S.: 'Highly efficient magnetically separable TiO₂-graphene oxide supported SrFe₁₂O₁₉ for direct sunlight-driven photoactivity', *Chem. Eng. J.*, 2014, **235**, pp. 264–274
- [34] Andrei J., Maria C., Aurelia M., Ileana R., Maria Z.: 'Influence of the silica based matrix on the formation of iron oxide nanoparticles in the Fe₂O₃-SiO₂ system, obtained by sol-gel method', *J. Mater. Chem.*, 2002, **12**, pp. 1401–1407
- [35] Hummers W.S., Offeman R.E.: 'Preparation of graphitic oxide', *J. Am. Chem. Soc.*, 1958, **80**, pp. 1339–1339
- [36] Kovtyukhova N.I., Ollivier P.J., Martin B.R., *ET AL.*: 'Layer-by-layer assembly of ultrathin composite films from micron-sized graphite oxide sheets and polycations', *Chem. Mater.*, 1999, **11**, pp. 771–778
- [37] Wang D.H., Choi D.W., Li J., *ET AL.*: 'Self-assembled TiO₂-graphene hybrid nanostructures for enhanced Li-ion insertion', *ACS Nano*, 2009, **3**, (4), pp. 907–914
- [38] Spurr R.A., Myers H.: 'Quantitative analysis of anatase-rutile mixtures with an X-ray diffractometer', *Anal. Chem.*, 1957, **29**, (5), pp. 760–762
- [39] Zhang H., Lv X., Li Y., Wang Y., Li J.: 'P25-graphene composite as a high performance photocatalyst', *ACS Nano*, 2010, **4**, (1), pp. 380–386
- [40] Yao Y., Li G., Ciston S., Lueptow R.M., Gray K.A.: 'Photoreactive TiO₂/carbon nanotube composites: synthesis and reactivity', *Environ. Sci. Technol.*, 2008, **42**, pp. 4952–4957
- [41] Zhang Y., Pan C.: 'TiO₂/graphene composite from thermal reaction of graphene oxide and its photocatalytic activity in visible light', *J. Mater. Sci.*, 2011, **46**, pp. 2622–2626
- [42] Li Q., Guo B., Yu J., *ET AL.*: 'Highly efficient visible-light-driven photocatalytic hydrogen production of CdS-cluster-decorated graphene nanosheets', *J. Am. Chem. Soc.*, 2011, **133**, pp. 10878–10884
- [43] Wang C., Cao M., Wang P., Ao Y., Hou J., Qian J.: 'Preparation of a magnetic graphene oxide-Ag₃PO₄ composite photocatalyst with enhanced photocatalytic activity under visible light irradiation', *J. Taiwan Inst. Chem. Eng.*, 2014, **45**, pp. 1080–1086
- [44] Mills A., Hunte S.L.: 'An overview of semiconductor photocatalysis', *J. Photochem. Photobiol., A*, 1997, **108**, pp. 1–35
- [45] Lihgtcap I.V., Kosel T.H., Kamat P.V.: 'Anchoring semiconductor and metal nanoparticles on a two-dimensional catalyst mat. storing and shuttling electrons with reduced graphene oxide', *Nano Lett.*, 2010, **10**, (2), pp. 577–583
- [46] Kamat P.V.: 'Graphene-based nanoassemblies for energy conversion', *J. Phys. Chem. Lett.*, 2011, **2**, (3), pp. 242–251